Performance of minimum energy controllers on tiltrotor aircraft

Tugrul Oktay
College of Aviation, Erciyes University, Kayseri, Turkey

Abstract

Purpose – The purpose of this article is to evaluate performance of minimum energy controllers thoroughly on a tiltrotor aircraft.

Approach – Minimum energy controllers are designed for tiltrotor aircraft models for helicopter and airplane modes. Performance of minimum energy controllers is evaluated with respect to several criteria.

Findings – Minimum energy controllers can be used for tiltrotor aircraft flight control system design. These controllers show satisfactory performance when noise intensities and variance bounds vary.

Practical implications – Minimum energy controllers can be implemented for tiltrotor aircraft flight control system design.

Originality/value – In this paper, minimum energy controllers are applied for tiltrotor aircraft flight control system design and the performance of minimum energy controllers is evaluated deeply on a complex physical system (i.e. tiltrotor aircraft).

Keywords Tiltrotor aircraft, Output variance constrained control, Minimum energy control, Closed-loop analysis

Paper type Research paper

Nomenclature

P, q, r	= aircraft angular velocities, [deg/s]
U, v, w	= aircraft linear velocities, [m/s]
ϕ_A, θ_A, ψ_A	= Aircraft Euler angles, [deg]
δ_{coll}, δ_{long}, δ_{lat}, δ_{ped} or u_1, u_2, u_3, u_4	= Collective, longitudinal stick, lateral stick and pedal perturbed pilot control inputs, [deg]
X	= State covariance matrix
ζ	= Convergence tolerance for controller design
a	= the scalar used to multiply with output variance bound
b	= the scalar used to multiply with noise intensities
E	= expectation operator
$\mathcal{J}$	= controller cost, []
n	= number of iteration for controller design
T	= matrix transpose
V	= sensor noise intensity and
W	= process noise intensity

Introduction

Tiltrotor aircrafts have been used in civil and military operations for important missions (e.g. search and rescue). The development of the tiltrotor aircraft models used in this article for control system design is presented in detail by Ferguson (1983), Klein (2006), Kleinhesselink (2007). Tiltrotor aircrafts experience many stability problems that make an efficient control system design essential. Recently, the technological advances succeeded in the area of control theory have contributed growth of the area of tiltrotor flight control system design. Advances in the tiltrotor technology were discussed in detail by Ford (1999).

Several control strategies have been applied on the tiltrotor aircraft flight control system throughout the years, such as classical Proportional-Integral-Derivative (PID) controllers (Papachristos *et al.*, 2011; Mattaboni *et al.*, 2012), modern control techniques based on matrix algebra linear matrix algebra, Linear Quadratic Regulator and Linear Quadratic Gaussian (LQG) approaches (Miller, 1991; Mattaboni *et al.*, 2012), H-inf control synthesis (Walker and Voskuijl, 2007; Yoo *et al.*, 2009), adaptive control techniques (Rysdyk *et al.*, 1997; Rysdyk and Calise, 1998; Rysdyk and Calise, 1999; Kendoul *et al.*, 2006; Krishnamurthy and Khorrami, 2011), Model Predictive Control (Nixon *et al.*, 2001), Higher Harmonic Control (Nixon *et al.*, 1997; Nixon *et al.*, 1998), Neural and Fuzzy Control (Rysdyk *et al.*, 1997; Zhu *et al.*, 2010; Chang *et al.*, 2012; Yu *et al.*, 2005; Kim *et al.*, 2010) and some other control aspects (Budiyono and Sutarto, 2004; Mueller *et al.*, 2006; Malpica *et al.*, 2012). In this article, a different control technique, namely, minimum energy controllers, is used for the tiltrotor aircraft flight control system design. Minimum energy controllers have been studied on other physical systems over the years such as hubble telescope (Skelton and Lorenzo, 1985), tensegrity structures (Skelton and Sultan, 1997a, 1997b) and helicopters (Oktay and Sultan, 2012a, 2012b, 2012c, 2012d; Oktay and Sultan, 2013). More research on minimum energy controllers to get better performance (e.g. disturbance rejection) have also been done recently (Baromand and Khaloozadeh, 2007; Baromand *et al.*, 2007; Khaloozadeh and Baromand, 2010).

The current issue and full text archive of this journal is available at **www.emeraldinsight.com/1748-8842.htm**

Aircraft Engineering and Aerospace Technology: An International Journal
86/5 (2014) 361–374

[DOI 10.1108/AEAT-11-2012-0225]

Aircraft Engineering and Aerospace Technology: An International Journal
Volume 86 · Number 5 · 2014 · 361–374

Minimum energy controllers have many advantages with respect to the other control approaches. First, these minimum energy controllers are improved LQG controllers, and they use Kalman filters as state estimators. Estimators are very important for complicated systems such as the tiltrotor aircraft, as some of the states of the linearized system cannot be easily measured. Second, second-order information (i.e. the state covariance matrix) is used for minimum energy controllers. It is crucial for multivariable control design, as all stabilizing controllers are parameterized in terms of this second-order information, which is physically meaningful. Finally, for strongly coupled, large Multi-Input Multi-Output (MIMO) systems, such as integration of minimum energy controllers and tiltrotor aircraft model in our work, the minimum energy controller design provides guarantees on the transient behavior of individual variables by enforcing upper bounds on the variance of these variables. Previous studies with minimum energy controllers revealed that they have lower controller cost than PID controllers (Skelton, 1987; Skelton *et al.*, 1998). Because the robustness of LQG controllers is not guaranteed, the requirement for robust control design, in fact, encouraged the control designers to use H-inf control synthesis. For H-inf control, robustness is certainly guaranteed; however, it has the disadvantage of the price of having to design an over-conservative controller. On the other hand, in the previous studies, robustness of minimum energy controllers on helicopter models is satisfied during flight condition uncertainties and inertial uncertainties, as well as both of these uncertainties (Oktay and Sultan, 2012a, 2012b, 2012c, 2012d; Oktay and Sultan, 2013). The nonlinear control theory is also used in the tiltrotor aircraft flight control system design, but the control designer has to deal with important difficulties such as implementation, computational hardness and robustness problems.

In this article, minimum energy controllers are applied on linearized tiltrotor aircraft models and their performance is deeply evaluated with respect to several criteria (i.e. sensitivity to noise intensity variation and variance bound variation). Closed-loop responses of the tiltrotor aircraft perturbed states and controls are also thoroughly examined with respect to these criteria. Both helicopter and aircraft modes are considered for these analyses.

This is the first article applying minimum energy controllers to the tiltrotor aircraft flight control system. One of the other important contributions of this article is in analyzing the performance of minimum energy controllers thoroughly on such a sophisticated system. Moreover, this is the first time closed-loop response analyses have been conducted using minimum energy controllers for tiltrotors.

Tiltrotor aircraft model

The tiltrotor aircraft model used in this article is presented by Ferguson (1983) in detail and summarized by Klein (2006) and Kleinhesselink (2007). This model captures fuselage, wings (left and right), horizontal stabilizer, vertical stabilizers (left and right), rotors (i.e. left and right) and rotor inflow. The blade flapping motion (i.e. collective and two cyclics) is also included in this model.

The key points of any tiltrotor aircraft are summarized next. The tiltrotor aircraft is neither a helicopter nor an aircraft, but it is combination of both. There are two main modes of the tiltrotor aircraft flight: helicopter and airplane modes. In the helicopter mode, the rotor shafts are pointed upward, similar to conventional helicopters, and the incidence angle is zero (Prouty, 2005). For the tiltrotor aircraft, longitudinal control (fuselage pitching motion) is obtained similar to that for helicopters by longitudinally tilting each rotor swashplate (i.e. left and right). Collective control is also obtained similar to a conventional helicopter by vertically moving the swashplate. Lateral and directional controls (fuselage roll and yaw motions) are the main differences between tiltrotors and helicopters. For helicopters, lateral control is obtained by laterally tilting the swashplate. On the other hand, for tiltrotors, it is made via differential collective inputs on each rotor. Directional control is obtained via differential longitudinal swashplate tilting for tiltrotors (Figure 1 for these rotor controls) and using tail rotor for helicopters. In the airplane mode, similar to conventional airplanes, longitudinal control is obtained using elevator and lateral control, which is obtained using differential movement of ailerons (it should be reminded that XV-15 has full-span flaps, and the ailerons are flaperons providing lateral control via differential movement). Directional control is obtained via movement of rudders. For more details and tiltrotor aircraft modeling discussion the references, Barkai *et. al.* (1998), Ford (1999), Maisel *et al.* (2000), Miller and Narkiewicz (2006), Yomchinda (2009), Yomchinda and Horn (2009) can also be examined.

Tiltrotor aircrafts have six rotor controls (i.e. three controls each for the left and right rotors, collective and two cyclics for each of the left and right rotors) and three airplane controls (i.e. aileron, elevator and rudder; Figure 1). For simplification, only pilot controls (i.e. collective, longitudinal and lateral sticks, pedal) are considered by Ferguson (1983). The XV-15 tiltrotor aircraft is used for the study of minimum energy controllers, and its configuration data can be found in

Figure 1 Helicopter and aircraft controls

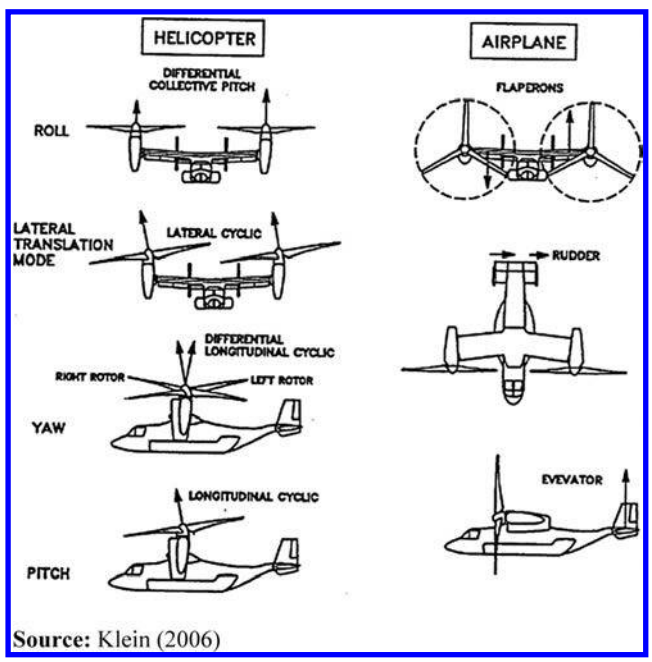

Source: Klein (2006)

Aircraft Engineering and Aerospace Technology: An International Journal
Volume 86 · Number 5 · 2014 · 361–374

the study by Ferguson (1983), Klein (2006), Kleinhesselink (2007).

The linear time-invariant (LTI) tiltrotor aircraft systems are in the following form:

$$\dot{x} = Ax + Bu \tag{1}$$

where , x and u are the perturbed states and control inputs (pilot controls). Matrices A and B are of size 9×9 and 9×4. The state and control vectors are $x = [u \;\; v \;\; w \;\; p \;\; q \;\; r \;\; \phi_A \;\; \theta_A \;\; \psi_A]^T$ and $u = [\delta_{coll} \;\; \delta_{long} \;\; \delta_{lat} \;\; \delta_{ped}]^T$, where u, v, w are perturbed linear velocity states; p, q, r are perturbed angular velocity states; ϕ_A, θ_A, ψ_A are perturbed Euler angle states; δ_{coll}, δ_{long}, δ_{lat} and δ_{ped} are collective, longitudinal stick, lateral stick and pedal perturbed pilot control inputs, respectively. In this article, for analyses, the XV-15 tiltrotor aircraft is chosen, and for hover flight condition (helicopter mode) and 200 kts straight-level flight condition (airplane mode), the A and B matrices are given in Appendix.

Minimum energy controllers

This article examines the specific minimum energy controller, namely, output variance constrained controller (OVC) (Skelton, 1987; Hsieh *et al.*, 1989; Zhu and Skelton, 1991; Skelton *et al.*, 1998). The OVC problem is summarized next. For a given continuous LTI system:

$$\dot{x} = Ax + Bu + Dw, \;\; y = Cx, \;\; z = Mx + v \tag{2}$$

and a positive definite input penalty (matrix or scalar) $R > 0$, find a full-order *dynamic* controller:

$$\dot{x}_c = A_c x_c + Fz, \;\; u = Gx_c \tag{3}$$

to solve the problem:

$$\min_{A_c,F,G} E_\infty \, u^T R u = tr(RGXG^T) \tag{4}$$

subject to:

$$E_\infty \, y_i^2 \le \sigma_i^2, \; i = 1, \ldots, n_y \tag{5}$$

From the above, y and z represent outputs of interest and sensor measurements, respectively; n_y is the number of outputs; wand and v are zero-mean uncorrelated Gaussian white noises with intensities of W and V, respectively; σ_i^2 is the upper bound imposed on the *i-th* output variance; x_c is the controller state vector; X is the state covariance matrix (Hsieh *et al.*, 1989; Zhu and Skelton, 1991); and F and G are state estimator matrix and controller gain matrix, respectively. Furthermore, *tr* denotes the matrix trace operator; *min* is the minimization operator; $E_\infty \triangleq \lim_{t\to\infty} E$; and E and T are expectation operator and matrix transpose operator, respectively. OVC solution reduces to an LQG problem solution by choosing the output penalty $Q > 0$, depending on the inequality constraints [i.e. equation (5]. An intelligent algorithm for the selection of Q is presented in Hsieh *et al.* (1989) and Zhu and Skelton (1991). OVC parameters, after converging on output penalty Q, are:

$$A_c = A + BG - FM, \;\; F = XM^T V^{-1}, \;\; G = -R^{-1}B^T K \tag{6}$$

where, X and K are solutions of two algebraic Riccati equations:

$$0 = XA^T + AX - XM^T V^{-1} MX + DWD^T \tag{7a}$$

$$0 = KA + A^T K - KBR^{-1}B^T K + C^T Q C \tag{7b}$$

In comparison with the classical LQG, in the specific minimum energy controller used in this article, namely, OVC, the penalty matrices Q and R are selected such that variance constraints on outputs of interest are satisfied, while the controller cost is minimized. In next two sections the Euler angles are outputs of interest, and the sensor measurements are all the perturbed states (i.e. linear and angular velocities and Euler angles). The inputs of interest are all perturbed control inputs. The measurement matrix is M = eye(9) and the output matrix (i.e. C) is the last three rows of matrix M.

Performance of minimum energy controllers

In this section, the performance of minimum energy controllers, specifically OVC, is deeply examined with respect to many criteria (i.e. sensitivity of output variances to magnitudes of noise intensities change, sensitivity of controller cost to magnitudes of noise intensities change, sensitivity of input variances to magnitudes of noise intensities change, sensitivity of controller cost to magnitudes of output variance bounds change and sensitivity of input variances to magnitudes of output variance bounds change).

Two flight conditions are considered to design OVC. The 1st flight condition is the helicopter mode (i.e. hover flight condition), and the 2nd flight condition is the airplane mode (i.e. 200 kts straight-level flight). For the 1st OVC, the outputs of interest were tiltrotor aircraft-perturbed Euler angle states (pitch, roll and yaw), while the inputs of interest were all four control inputs. The magnitude of variance bounds on the Euler angle states was $\sigma^2_{(\phi_A,\,\theta_A,\,\psi_A)} = 10^{-4}[1 \;\; 1 \;\; 10]$. The additional OVC algorithm parameters to run the code were $n = 100$ and $\zeta = 10^{-5}$, where n is the maximum allowable iteration number and ζ is the convergence tolerance. MATLAB is used to run the code. After 12 iterations, the OVC algorithm converged and satisfied the output constraint with a convergence error of 5.99×10^{-6}. The controller cost for this design was 0.15 [equation (4)].

The 2nd OVC is designed for the 2nd flight condition (i.e. 200 kts straight-level flight, tiltrotor airplane mode). The only different design parameter for the 2nd OVC from the previous OVC is that the magnitude of variance bounds on Euler angle states was $\sigma^2_{(\phi_A,\,\theta_A,\,\psi_A)} = 10^{-4}[2 \;\; 2 \;\; 20]$. After 16 iterations, the OVC algorithm converged and satisfied the output constraint with a convergence error of 9.77×10^{-6}. The controller cost for the design of the 2nd OVC was 0.022. In the next subsections, the performance of OVC for two tiltrotor modes (i.e. helicopter and airplane modes) is examined.

The state estimator and controller gain matrices are given in Appendix for 1st and 2nd OVCs.

Helicopter mode (hover flight condition)

In this subsection, the tiltrotor aircraft model, which is linearized around hover flight condition, is used. In Figure 2, the sensitivity of output variances to magnitudes of noise

Aircraft Engineering and Aerospace Technology: An International Journal
Volume 86 · Number 5 · 2014 · 361–374

Figure 2 Sensitivity of output variances and controller cost to magnitudes of noise intensities change

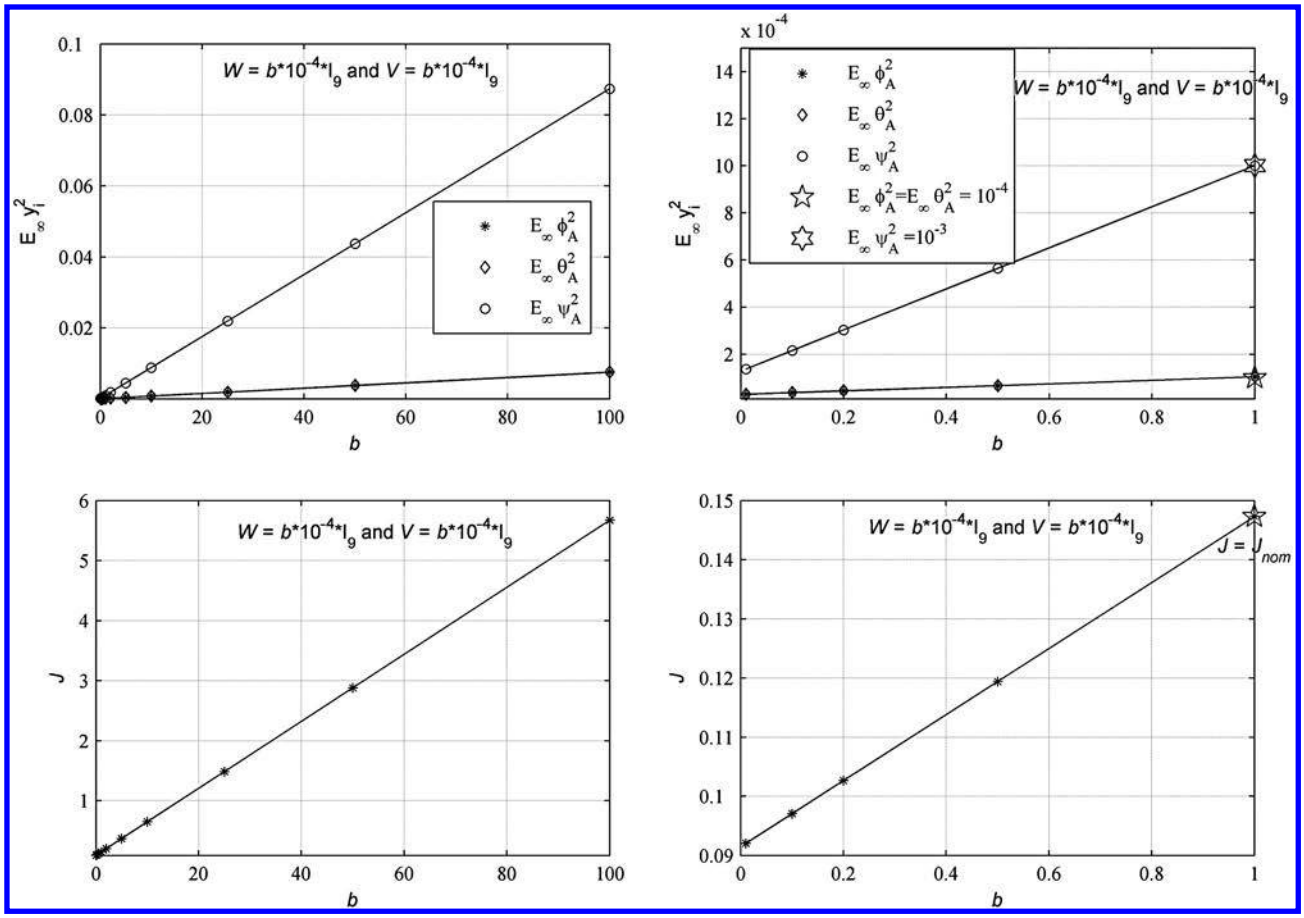

intensities change is shown. In this figure, the 1st OVC is used, and the controller parameters [state estimator and controller gain; equation (6)] are fixed. The linear tiltrotor model [A, B, C and M matrices; equation (2)] is also fixed. The altering parameters are intensities of process and measurement noises (i.e. W and V). These intensities are multiplied with a scalar, b, simultaneously, and the behavior of output variances is shown in Figure 2. It can be seen from this figure that there is a linear relationship between the magnitudes of b and output variances (i.e. $E_\infty\phi_A^2$, $E_\infty\theta_A^2$, $E_\infty\psi_A^2$). As the magnitude of b increases, the magnitudes of output variances increases in a linear fashion.

In Figure 2, the sensitivity of controller cost to magnitudes of noise intensities change is also given. From Figure 2, it can also be easily seen that when the magnitude of b increases, the amount of controller cost increases linearly. In this figure, $\mathcal{J}_{nom}$ is the nominal controller cost, which is obtained using $b = 1$.

In Figure 3, the sensitivity of input variances to magnitudes of noise intensities change is shown. Because the variance of the 2nd input is relatively too small with respect to other inputs, it is given separately. In Figure 3, the varying parameters are the same as those of the previous figure (i.e. W and V). From Figure 3, it can be concluded that when noise intensities are multiplied with b simultaneously, the magnitudes of input variances increase in a roughly linear fashion. In this figure, $[E_\infty u_i^2]_{nom}$ shows the nominal variance value-related input.

In Figure 4, a different scenario is examined. In the previous example, the control system parameters [F and G; equation (6)] and linear model parameters [A, B, C and M matrices; equation (2)] were fixed, while the noise intensities (i.e. W and V) were altering simultaneously with multiplication scalar, b. However, in this figure, the linear model parameters and noise intensities are fixed, while the output variance bound for the OVC design is changed. In this figure, the logarithmic scale is used, as the controller cost and input variances are too large when the output constraint is too tight ($a < 0.5$). Variance bound of each output of interest (i.e. yaw, pitch and roll states) is multiplied with scalar, a, and for each output constraint bound (i.e. the ones found after multiplication with scalar a), a new OVC is designed with the same code summarized at the beginning of this section. In Figure 4, $\log_{10}$ is referring to logarithm to the base of 10. In Figure 4, the sensitivity of controller cost and input variances to magnitude of output variance bound change is given, and from this figure, it can be concluded that the controller cost and input variances increase in a rough exponential fashion as the multiplication scalar a decreases. The increases of input variances with decreasing a explain why controller cost also increases with decreasing a. It should be reminded that the input variances and controller cost change in the same direction (Skelton, 1987; Skelton *et al.*, 1998).

Aircraft Engineering and Aerospace Technology: An International Journal
Volume 86 · Number 5 · 2014 · 361–374

Figure 3 Sensitivity of input variances to magnitudes of noise intensities change

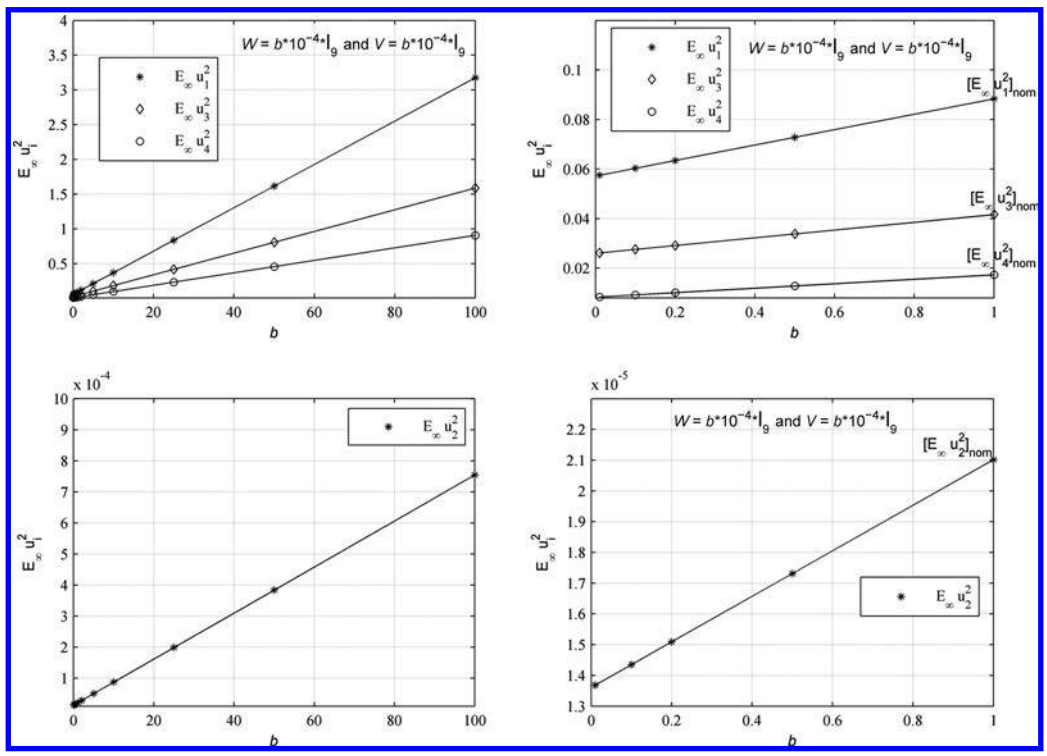

Airplane mode (200 kts straight-level flight condition)
In this subsection, the tiltrotor aircraft model which is linearized around 200 kts straight-level flight condition (airplane mode) is used. In Figure 5, the sensitivity of output variances and controller cost to magnitudes of noise intensities change is given, and a similar study with Figure 2 is done. In addition, in this example, the controller parameters [F and G matrices; equation (6)] and linear tiltrotor model [A, B, C and M matrices; equation (2)] are fixed. The differences between Figure 2 and Figure 5 are control system parameters (F and G matrices, 1st OVC for Figure 2 and 2nd OVC for Figure 5) and linear aircraft model (A and B matrices). It can be also concluded from Figure 5 that output variances (i.e. $E_\infty\phi_A^2$, $E_\infty\theta_A^2$, $E_\infty\psi_A^2$) and controller cost increase in a linear fashion with increasing b.

In Figure 6, the sensitivity of input variances to magnitudes of noise intensities change is given. The linearized model and control system parameters in this figure are similar to those in Figure 5. The differences between Figures 2 and 5 are also similar to the ones between Figures 3 and 6. From Figure 6, it can be easily concluded that the magnitudes of input variances change linearly with increasing b.

In Figure 7, a different situation is studied. In the previous examples of this subsection (Figures 5 and 6), the control system parameters (F and G) and linear model parameters (A, B, C and M matrices) were fixed, while the noise intensities (W and V) were multiplied with b. On the other hand, in Figure 7, the linear model parameters and noise intensities are fixed ($b = 1$), while the output variance that is bound for OVC design varies. The study done in this figure is similar with the one in Figure 4. In Figure 7, the sensitivity of controller cost and input variances to magnitude of output variance bound change is given, and from this figure, it can be safely said that the amount of controller cost and input variances increases exponentially with decreasing a.

Figure 7 Sensitivity of controller cost and input variances to magnitude of output variance bound change.

Simulation results

In this section, the performance and sensitivity of closed-loop responses of outputs of interest (i.e. Euler angle states), other outputs (i.e. linear and angular velocity states) and all inputs to noise intensities (i.e. W and V) variation are investigated. For this purpose, both process and measurement noise intensities are multiplied with a scalar constant, b, simultaneously. The performance and sensitivity of closed-loop responses of all outputs and inputs to output variance bound ($\sigma^2_{(\phi_A,\,\theta_A,\,\psi_A)}$) variation is also studied. To perform this analysis, output variance bound to design OVC (i.e. output variance-constrained controller) is multiplied with a scalar constant, a. For both of these studies, two linearized models are used (i.e. the ones linearized around the hover flight condition and 200 kts straight-level flight condition).

The closed-loop systems are created using a dynamic control system (i.e. OVC designed for the linear tiltrotor aircraft model) and coupled to a dynamic system (i.e. linear tiltrotor aircraft model). Closed-loop systems are also excited by white noise perturbations of intensities W and V.

Helicopter mode (hover flight condition)
In this subsection, the tiltrotor aircraft model which is linearized around the hover flight condition is used. In Figure 8, the sensitivity of closed-loop responses of outputs of

Figure 4 Sensitivity of controller cost and input variances to magnitude of output variance bound change

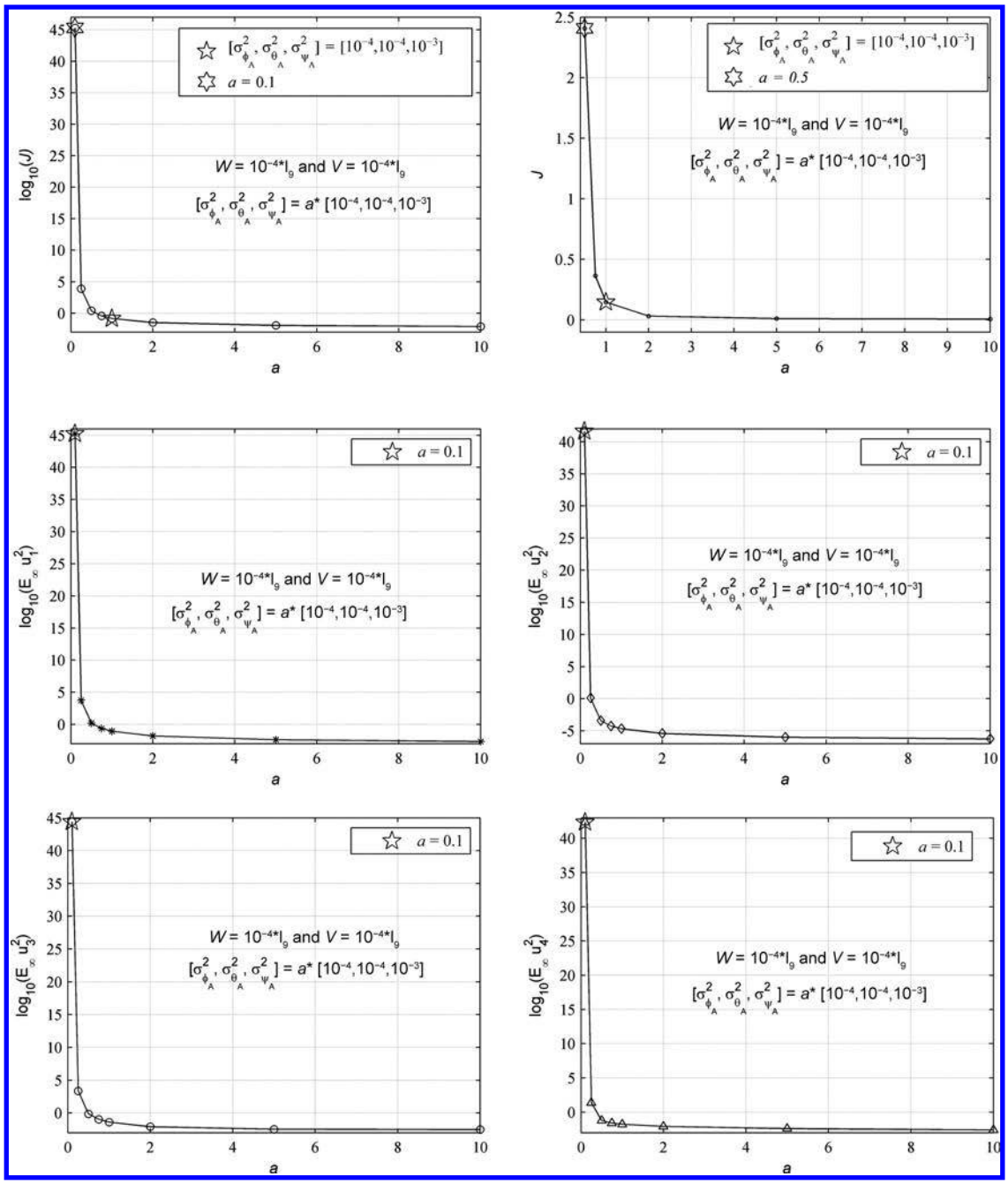

interest (i.e. Euler angle states) to magnitudes of noise intensities variation is given. The closed-loop system used for this figure is obtained by using OVC designed for tiltrotor aircraft model linearized around hover flight condition with variance bound of $\sigma^2_{(\phi_A, \theta_A, \psi_A)} = 10^{-4}[1\ \ 1\ \ 10]$ (i.e. the 1st OVC) and the tiltrotor aircraft model linearized around the hover flight condition. This closed-loop system is also excited by the process and measurement intensities of W and V, respectively. In Figure 8, the varying parameters are white noise perturbations of intensities W and V, and these intensities are multiplied with a scalar, b, simultaneously. In this figure, closed-loop responses of Euler angle states (i.e. ϕ_A :roll, θ_A :pitch, ψ_A :yaw) are given, while noise intensities are simultaneously multiplied with $b = 1$ (solid black line), $b = 0.1$ (solid pale purple line) and $b = 10$ (solid cyan line). From Figure 8, it can be easily seen that the peak values of Euler angles increase as the multiplication scalar, b, increases.

In Figure 8, the closed-loop responses of outputs of interest are also given when $b = 1$. From this part of figure, it can be concluded that the peak value of any output increases with increasing variance bound. In this part of figure, the largest variance bound is on the yaw angle state, and its peak of value is the maximum among all Euler angle states.

Aircraft Engineering and Aerospace Technology: An International Journal
Volume 86 · Number 5 · 2014 · 361–374

Figure 5 Sensitivity of output variances and controller cost to magnitudes of noise intensities change

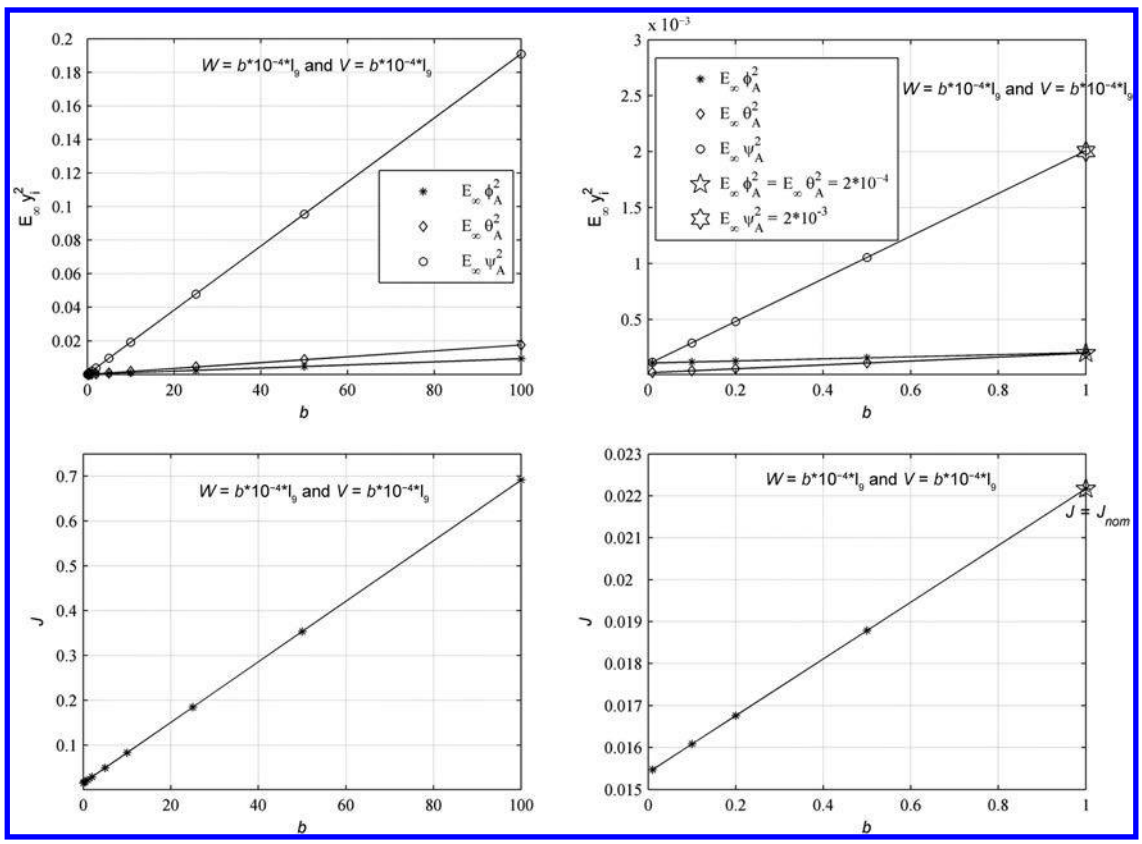

Figure 6 Sensitivity of input variances to magnitudes of noise intensities change

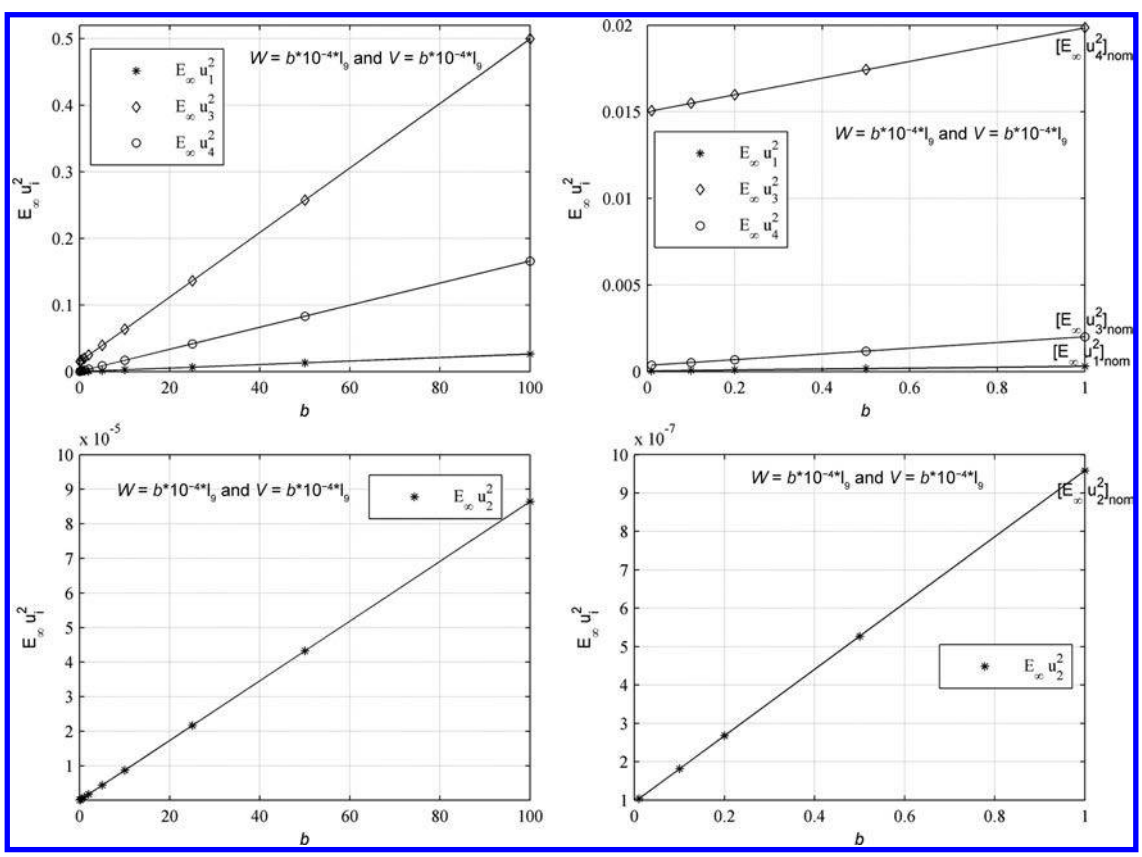

Figure 7 Sensitivity of controller cost and input variances to magnitude of output variance bound change

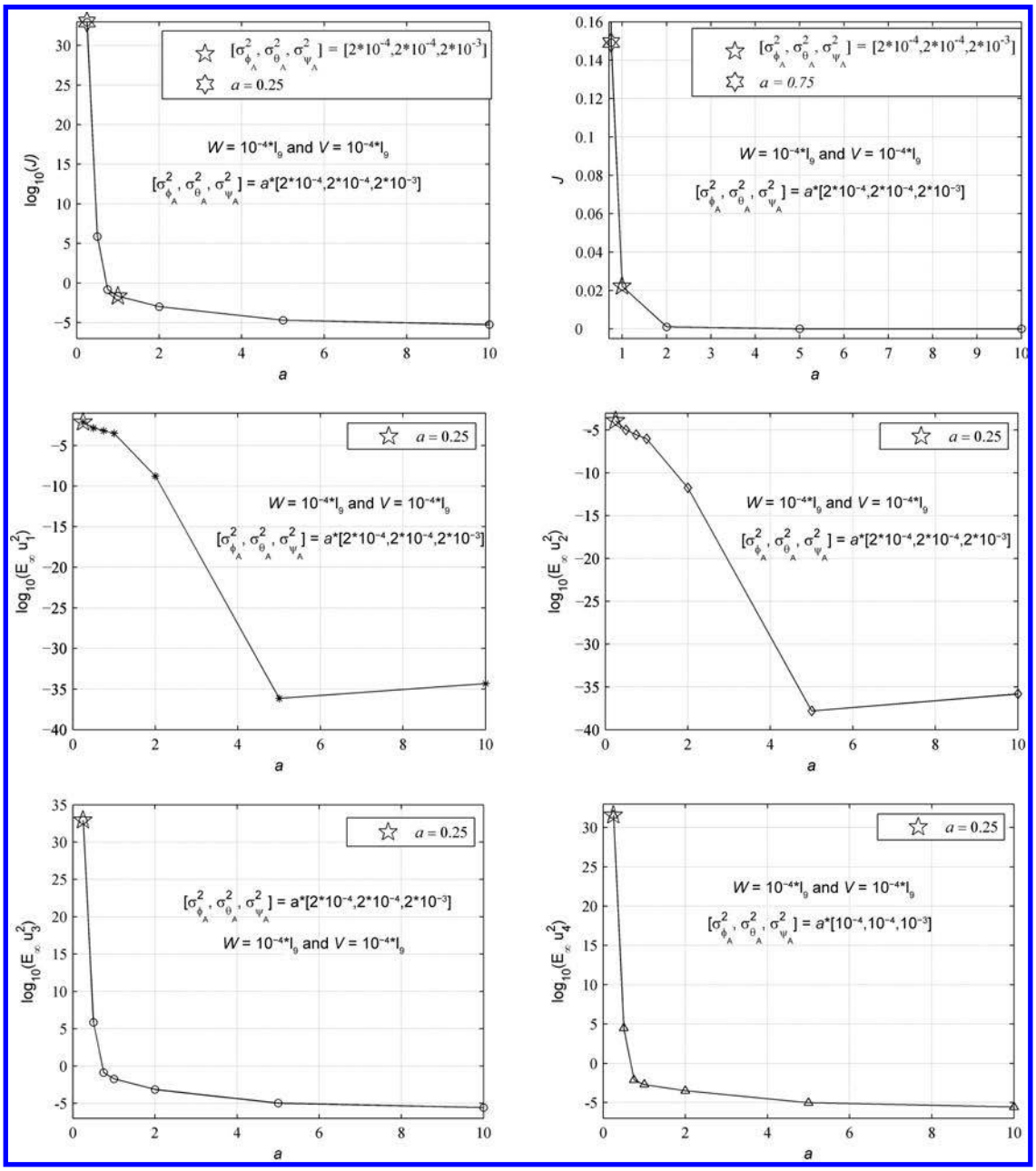

In Figure 9, the sensitivity of closed-loop responses of some other outputs (i.e. some linear and angular velocity states) and some inputs of interest (collective and longitudinal sticks) to magnitudes of noise intensities variation is shown. The closed-loop system used for simulation results is the same with the one used in the previous example. Solid black, pale purple and cyan colors refer the situations of b = 1, b = 0.1 and b = 10, respectively. In addition, using extensive analyses from this figure, it can be seen that the other outputs (the ones which are not used for OVC design) do not experience fast and large variations. Their peak values increase as the magnitudes of noise intensities increase. The peak values of inputs increase with increasing multiplication scalar, b, and the second input is less effective than other inputs while controlling the closed-loop system.

In Figure 10, the sensitivity of closed-loop responses of outputs of interest to magnitude of output variance bound variation is shown. In this figure, a different situation is studied. The control system (i.e. OVC) changes with a multiplication scalar, a. The closed-loop system changes with altering a. In this example, three different closed-loop systems are obtained for a = 1, a = 0.5 and a = 2. From Figure 10, it can be easily seen that the peak values of closed-loop responses of Euler angle states increase with increasing multiplication scalar, a.

In Figure 11, the sensitivity of closed-loop responses of some other outputs (i.e. some linear and angular velocity

Figure 8 Sensitivity of closed-loop responses of outputs of interest to magnitudes of noise intensities variation

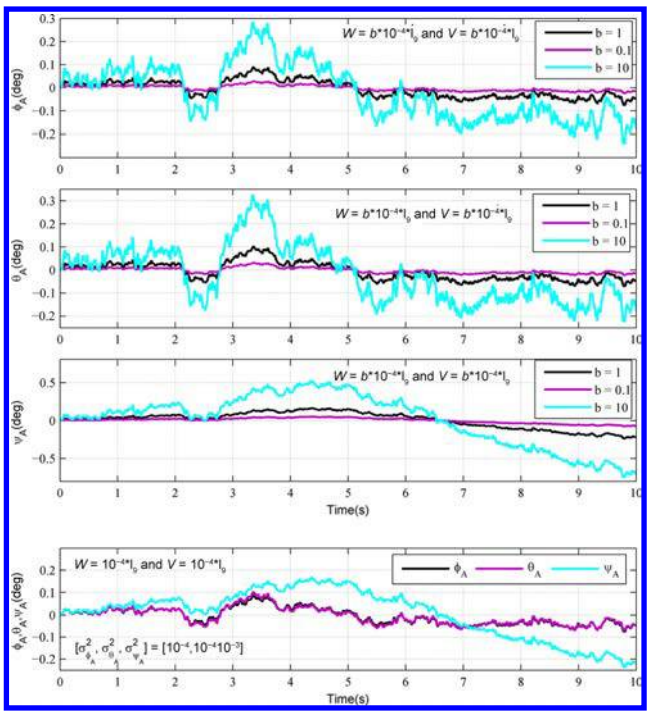

states) and some inputs of interest (collective and longitudinal sticks) to magnitude of output variance bound variation is given. In this example, the closed-loop systems used for simulation results are the same with the ones used in the previous example. Using extensive analyses, it can be concluded from Figure 11 that the peak values of linear velocity states (i.e. u, v, w) increase as the multiplication scalar a increases. On the other hand, the peak values of angular velocities (i.e. p, q, r) decrease with increasing a. Moreover, the peak values of all the inputs decrease with increasing multiplication scalar, a, and the result can be explained by the fact that when the output variance bound to design an OVC becomes smaller, the amount of inputs (Skelton, 1987; Skelton *et al.*, 1998) becomes larger.

Airplane mode (around 200 kts straight-level flight condition)

In this subsection, the tiltrotor aircraft model which is linearized around 200 kts straight-level flight condition is used. In Figure 12, the sensitivity of closed-loop responses of outputs of interest (i.e. Euler angle states) to magnitudes of noise intensities variation is given. In this figure, the closed-loop system obtained by using OVC designed for the tiltrotor aircraft model linearized around 200 kts straight-level flight condition with variance bound of $\sigma^2_{(\phi_A,\,\theta_A,\,\psi_A)} = 10^{-4}\,[2\quad 2\quad 20]$ (i.e. the 2nd OVC) and the tiltrotor aircraft model linearized around 200 kts straight-level flight condition is used. This closed-loop system is also excited by process and measurement intensities. In Figure 12, the changing quantities are noise intensities, and they are multiplied with b simultaneously. In this figure, closed-loop responses of Euler angle states are given, while noise intensities are

Figure 9 Sensitivity of closed-loop responses of some other outputs and inputs of interest to magnitudes of noise intensities variation

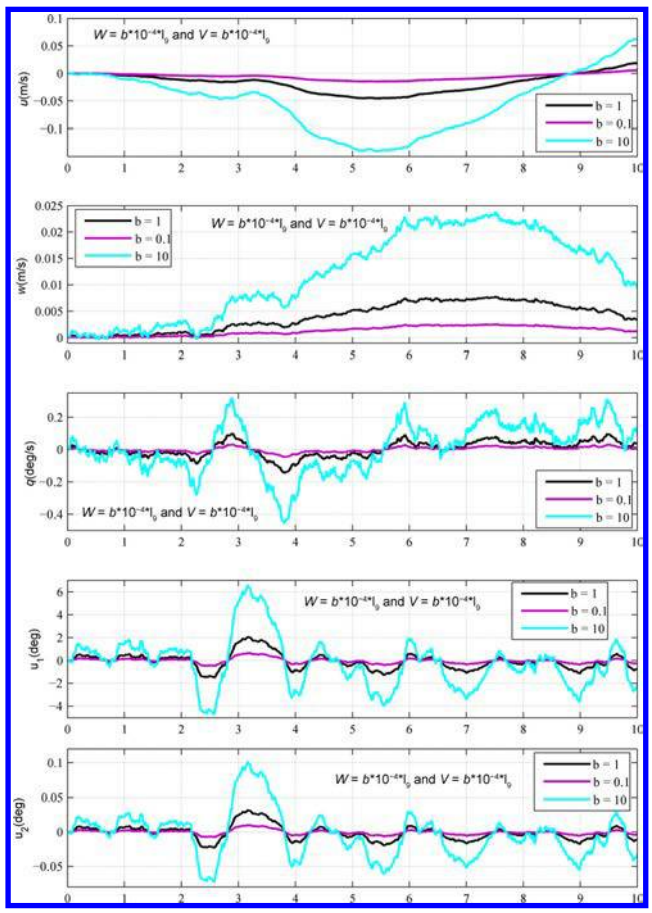

Figure 10 Sensitivity of closed-loop responses of outputs of interest to magnitude of output variance bound variation

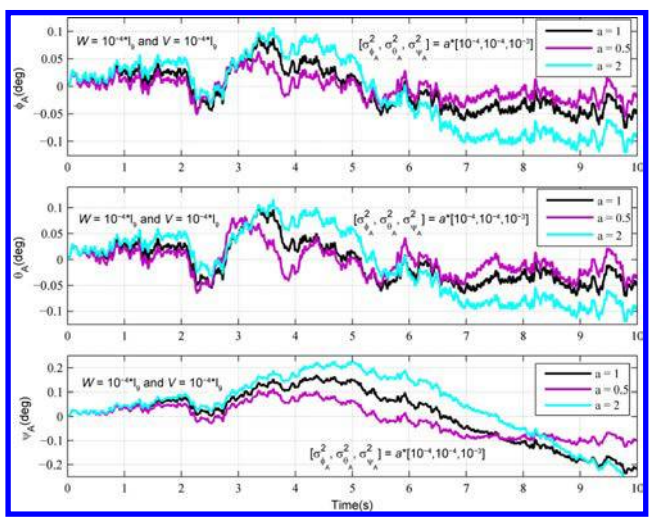

simultaneously multiplied with $b = 1$ (solid black line), $b = 0.1$ (solid pale purple line) and $b = 10$ (solid cyan line). From Figure 12, the same result with Figure 8, it can be concluded that when the multiplication scalar b increases, the peak values of Euler angles increase.

Aircraft Engineering and Aerospace Technology: An International Journal
Volume 86 · Number 5 · 2014 · 361–374

Figure 11 Sensitivity of closed-loop responses of some other outputs and inputs of interest to magnitude of output variance bound variation

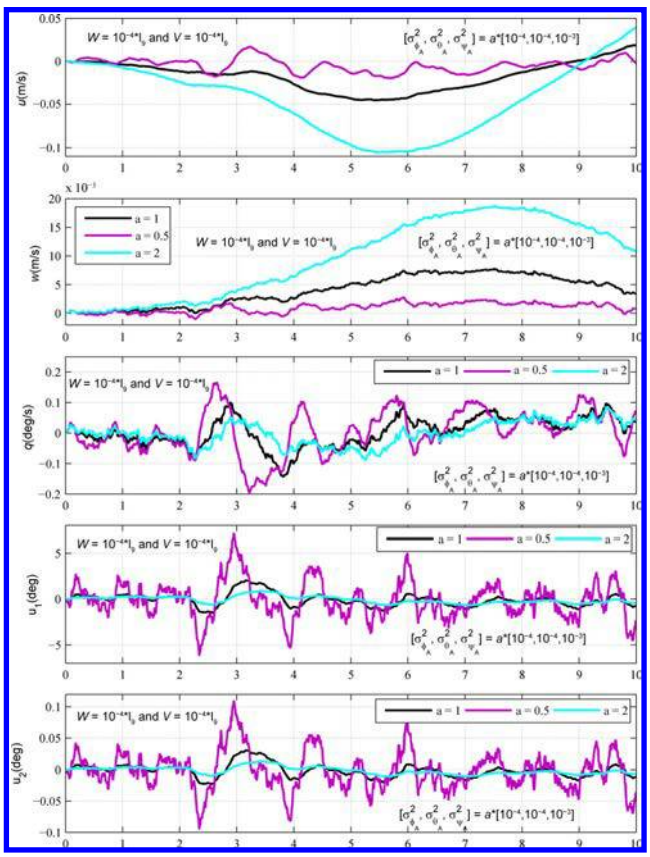

Figure 12 Sensitivity of closed-loop responses of outputs of interest to magnitudes of noise intensities variation

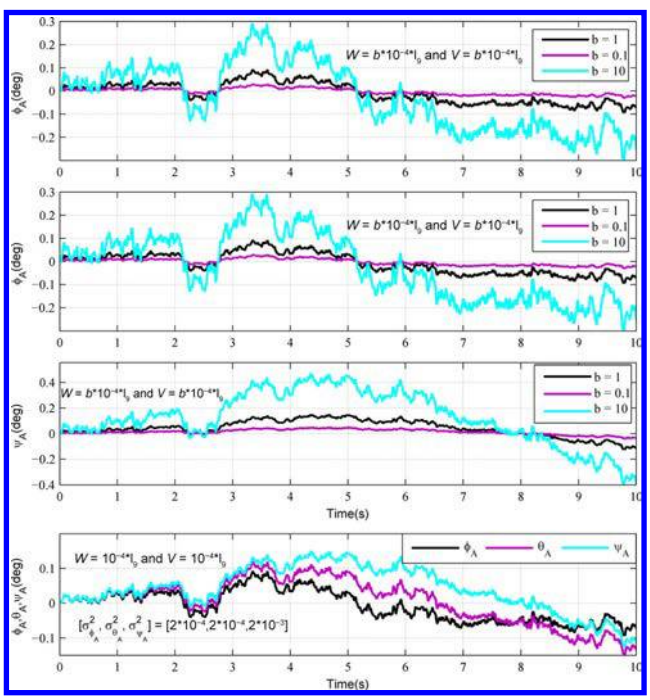

In Figure 12, the closed-loop responses of outputs of interest are also shown while $b = 1$. From this part of figure, it can easily be seen that the peak value of the yaw angle state (solid cyan line) is the maximum among all three Euler angle states, as the variance bound on it is the maximum ($\sigma^2_{\psi_A} = 2*10^{-3}$).

In Figure 13, the sensitivity of closed-loop responses of some other outputs (i.e. the outputs which are not considered for the control system design) and some inputs of interest (collective and longitudinal sticks) to magnitudes of noise intensities variation is shown. The closed-loop system used in this example is obtained similarly as the one used in the previous example. Using extensive analyses from Figure 13, it can be easily seen that the other outputs (i.e. linear and angular velocity states) do not experience catastrophic behavior (i.e. fast and large variations). The peak values of other outputs increase with increasing b. It arrived at the conclusion similar to that in Figure 9 that as b increases, the peak values of inputs increase.

In Figure 14, the sensitivity of closed-loop responses of outputs of interest (i.e. Euler angle states) to magnitude of output variance bound variation is shown. In this figure, the closed-loop system changes with altering a. From Figure 14, it can be ascertained that as a increases, the peak values of closed-loop responses of Euler angle states increase.

In Figure 15, the sensitivity of closed-loop responses of some other outputs (i.e. the outputs which are not considered for control system design) and some inputs of interest (collective and

Figure 13 Sensitivity of closed-loop responses of some other outputs and inputs of interest to magnitudes of noise intensities variation

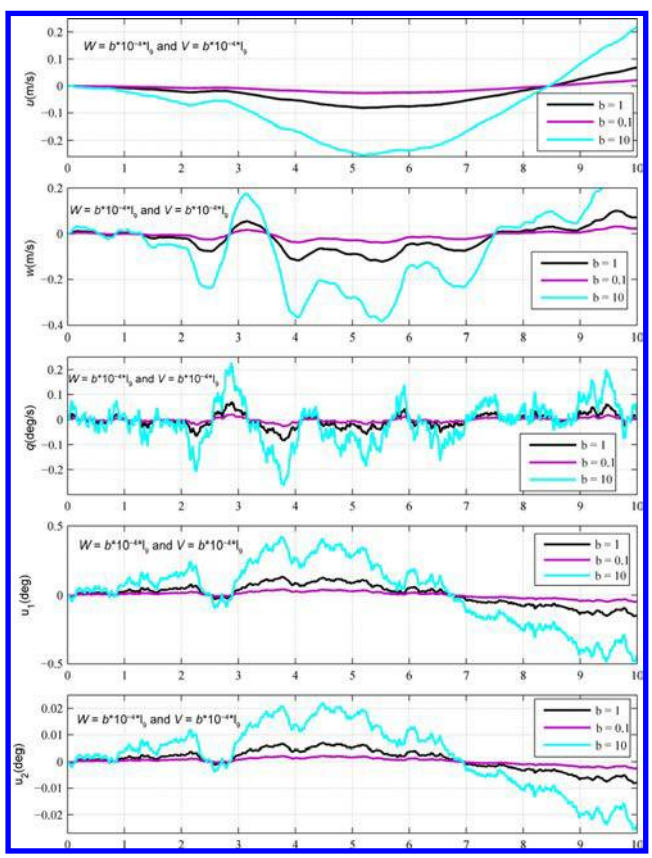

Aircraft Engineering and Aerospace Technology: An International Journal
Volume 86 · Number 5 · 2014 · 361–374

Figure 14 Sensitivity of closed-loop responses of outputs of interest to magnitude of output variance bound variation

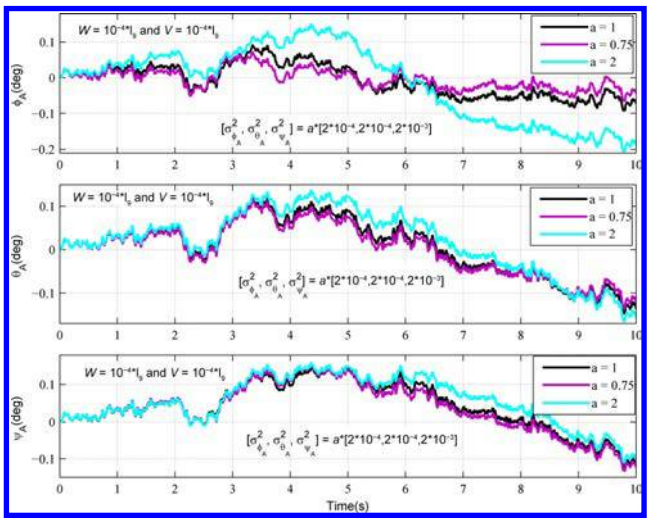

Figure 15 Sensitivity of closed-loop responses of some other outputs to magnitude of output variance bound variation

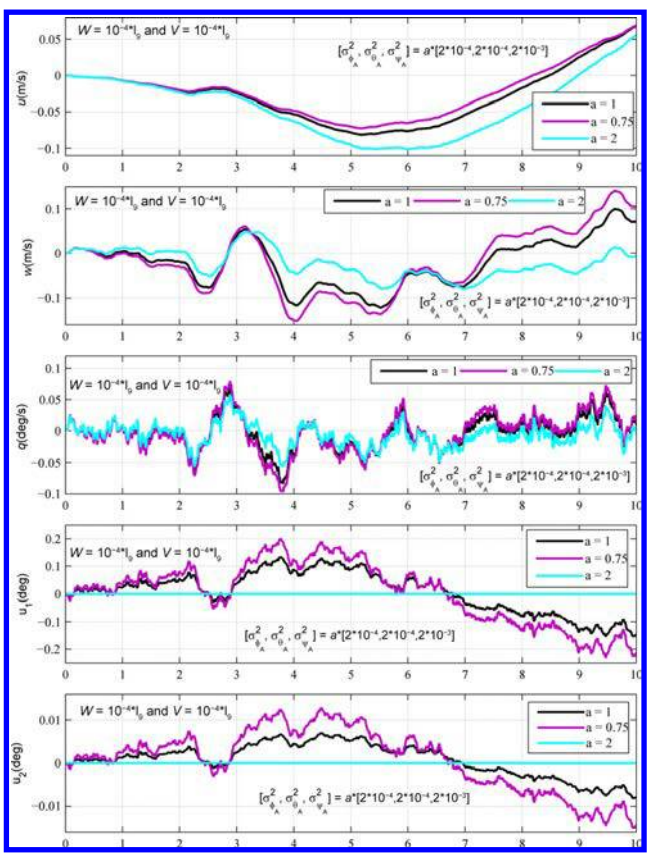

longitudinal sticks) to magnitude of output variance bound variation is given. The closed-loop systems used for this example are the same with the ones used in the previous example. It should be reminded that there are three controllers (for $a = 1$, $a = 0.75$ and $a = 2$); therefore, there are three control systems (i.e. OVCs). Using extensive analyses from Figure 15, it can be seen that the other outputs (i.e. linear and angular velocities) do not experience catastrophic behavior when a varies, and when a increases, the peak values of all the inputs decrease. When $a = 2$, the 1st and 2nd inputs seem ineffective. This is due to the too low input variance values after designing OVC with $a = 2$.

Conclusions

Linear tiltrotor aircraft models capturing helicopter and airplane modes are used for the design of minimum energy controllers, specifically OVCs. The performance of OVCs is thoroughly examined with respect to several criteria (i.e. sensitivity to noise intensity variation and variance bound variation). Closed-loop responses of perturbed states and controls are studied when noise intensities and variance bound for OVC design change.

Similar results are found for helicopter and airplane modes. For fixed OVC, the magnitudes of input and output variances and the amount of controller cost increase in a linear fashion with increasing magnitudes of noise intensities. While OVC changes due to the variation of output variance bound, the controller cost and input variances increase in an exponential fashion with decreasing magnitude of the output variance bound. Closed-loop response studies demonstrate that for a fixed tiltrotor flight control system (i.e. OVC), the peak values of Euler angle states (i.e. outputs of interest) and inputs increase with increasing magnitudes of noise intensities, and when OVC changes, the peak values of Euler angle states increase with increasing magnitude output variance bound. On the other hand, the peak values of inputs decrease as the output variance bound increases. Moreover, any output and input do not experience fast and large variations in both situations (i.e. for the cases of noise intensity variation and variance bound variation).

References

Barkai, S.M., Rand, O., Peyran, R.J. and Carlson, R.M. (1998), "Modeling and analysis of tilt-rotor aeromechanical phenomena", *Mathematical and Computer Modeling*, Vol. 27 No. 12, pp. 17-43.

Baromand, S. and Khaloozadeh, H. (2007), "Output covariance tracking of linear stochastic systems", *Mediterranean Conference on Control and Automation*, *Athens*, pp. 1-6.

Baromand, S., Khaloozadeh, H. and Rajati, M. (2007), "Output covariance tracking as a disturbance rejection problem", *46th IEEE Conference on Decision and Control*, *New Orleans, LA*.

Budiyono, A. and Sutarto, H.Y. (2004), "Controller design for a VTOL Aircraft: a case study of coefficient diagram method application for a time-varying system", *Regional Conference on Aeronautical Science, Technology and Industry*, *Bandung*.

Chang, S.H., Bang, H.C., Lee, W.S. and Park, B.J. (2012), "Dynamic modeling and fuzzy control for a small tiltrotor unmanned aerial vehicle", *Proceedings of the Institution of Mechanical Engineers, Part G, Journal of Aerospace Engineering*, Vol. 228 No. 10, pp. 1468-1487.

Ferguson, S.W. (1983), "A mathematical model for real time flight simulation of a generic tilt-proprotor aircraft", NASA-CR-166536.

Ford, T. (1999), "Tiltrotor progress", *Journal of Aircraft Engineering and Aerospace Technology*, Vol. 71 No. 1, pp. 42-47.

Hsieh, C., Skelton, R.E. and Damra, F.M. (1989), "Minimum energy controllers with inequality constraints on output variances", *Optimal Control Application and Methods*, Vol. 10 No. 4, pp. 347-366.

Juhasz, O., Roberto, C., Ivler, C.M, Tischler, M.B and Berger, T. (2012), "Flight dynamic simulation modeling of large flexible tiltrotor aircraft", *American Helicopter Society 68th Annual Forum*, ForthWorth, TX.

Kendoul, F., Fantoni, I. and Lozano, R. (2006), "Modeling and control of a small autonomous aircraft having two tilting rotors", *IEEE Transactions of Robotics*, Vol. 22 No. 6, pp. 1297-1302.

Khaloozadeh, H. and Baromand, S. (2010), "State covariance assignment problem", *IET Control Theory and Applications*, Vol. 4 No. 3, pp. 391-402.

Kim, B.M., Kim, B.S. and Kim, N.W. (2010), "Trajectory tracking controller design using neural networks for a tiltrotor unmanned aerial vehicle", *Proceedings of the Institution of Mechanical Engineers, Part G, Journal of Aerospace Engineering*, Vol. 224 No. 8, pp. 881-896.

Klein, G.D. (2006), "Linear modeling of tiltrotor aircraft", MS thesis, Naval Postgraduate School, CA.

Kleinhesselink, K.M. (2007), "Stability and control modeling of tiltrotor aircraft", MS thesis, University of Maryland, MD.

Krishnamurthy, P. and Khorrami, F. (2011), "Adaptive back stepping and θ-D based controllers for a tilt-rotor aircraft", *19th International Conference on Control and Automation*, *Corfu*.

Maisel, M.D., Giulianetti, D.J. and Dugan, D.C. (2000), "The history of the XV-15 tiltrotor research aircraft – from concept to flight", NASA SP-2000-4517.

Malpica, C.A., Lawrence, B. and Lindsey, J. (2012), "Handling qualities of a large civil tiltrotor in hover using translational rate command", *American Helicopter Society 68th Annual Forum*, ForthWorth, TX.

Mattaboni, M., Masarati, P., Quaranta, G. and Mantegazza, P. (2012), "Multibody simulation of integrated tiltrotor flight mechanics, aeroelasticity, and control", *Journal of Guidance, Control and Dynamics*, Vol. 35 No. 5, pp. 1391-1405.

Miller, D.G. (1991), "Tiltrotor Control law design for rotor loads alleviation using modern control techniques", *American Control Conference*, *Philadelphia, PA*.

Miller, M. and Narkiewicz, J. (2006), "Tiltrotor modeling for simulation in various flight conditions", *Journal of Theoretical and Applied Mechanics*, Vol. 44 No. 4, pp. 881-906.

Mueller, J.P., Gourinat, Y., Ferrer, R., Krysinski, T. and Kerdreux, B. (2006), "A numerical study on active control for tiltrotor whirl flutter stability augmentation", *Journal of American Helicopter Society*, Vol. 51 No. 3, pp. 244-254(11).

Nixon, M.W., Langston, C.W., Singleton, J.D., Piatak, D.J., Kvaternik, R.G., Bennett, R.L. and Brown, R.K. (2001), "Experimental investigation of generalized predictive control for tiltrotor stability augmentation", *CEAS/AIAA/AIAE International Forum of Aeroelasticity and Structural Dynamics*, Madrid.

Nixon, M.V., Kvaternik, R.G. and Settle, T.B. (1997), "Higher harmonic control for tiltrotor vibration reduction", *CEAS International, Forum on Aeroelasticity and Structural Dynamics*, Rome.

Nixon, M.V., Kvaternik, R.G. and Settle, T.B. (1998), "Tiltrotor vibration reduction through higher harmonic control", *Journal of American Helicopter Society*, Vol. 43 No. 3, pp. 235-245(11).

Oktay, T. and Sultan, C. (2012a), "Variance constrained control of manuvering helicopters", *American Helicopter Society 68th Annual Forum*, Forth Worth, TX.

Oktay, T. and Sultan, C. (2012b), "Integrated maneuvering helicopter model and controller design", *Proceedings of AIAA Guidance Navigation and Control Conference*, *Minneapolis, MN*.

Oktay, T. and Sultan, C. (2012c), "Variance constrained control of maneuvering helicopters with sensor failure", *Proceedings of the Institution of Mechanical Engineers, Part G, Journal of Aerospace Engineering*, Vol. 227 No. 12, pp. 1845-1858.

Oktay, T. and Sultan, C. (2012d), "Simultaneous helicopter and control system design", *AIAA Journal of Aircraft*, Vol. 50 No. 3, pp. 911-925.

Oktay, T. and Sultan, C. (2013), "Modeling and control of a helicopter slung-load system", *Aerospace Science and Technology*, Vol. 29 No. 1, pp. 206-222.

Papachristos, C., Alexis, K. and Tzes, A. (2011), "Design and experimental attitude control of an unmanned tilt-rotor aerial vehicle", *15th International Conference on Advanced Robotics*, *Tallinn*.

Prouty, R.W. (2005), *Helicopter Performance, Stability and Control*, in Robert, E. (Ed.), Kreiger Publishing Company, Melbourne, FL, pp. 488-489.

Rysdyk, R.T. and Calise, A.J. (1998), "Adaptive nonlinear control for tiltrotor aircraft", *Proceedings of the IEEE International Conference on Control Applications*, *Trieste*.

Rysdyk, R.T. and Calise, A.J. (1999), "Adaptive model inversion flight control for tilt-rotor aircraft", *Journal of Guidance, Control, and Dynamics*, Vol. 22 No. 3, pp. 402-407.

Rysdyk, R.T., Calise, A.J. and Chen, R.T.N. (1997), "Nonlinear adaptive control of tiltrotor aircraft using neural networks", *SAE Transactions*, Vol. 106, pp. 1809-1816.

Skelton, R.E. (1987), *Linear Systems Analysis and Synthesis*, Chapter 8, Dynamic Systems Control, John Wiley & Sons, New York.

Skelton, R.E. and Lorenzo, M.D. (1985), "Space structure control design by variance assignment", *Journal of Guidance, Control and Dynamics*, Vol. 8 No. 4, pp. 454-462.

Skelton, R.E. and Sultan, C. (1997), "Controllable tensegrity, a new class of smart structures", *International Symposium on Smart Structures and Materials*, San Diego, CA.

Skelton, R.E., Iwasaki, T. and Grigoriadis, K. (1998), *A Unified Algebraic Approach to Linear Control Design*, Chapter 4, Taylor & Francis, London, ISBN 07484 0592 5.

Sultan, C. and Skelton, R.E. (1997), "Integrated design of controllable tensegrity structures", *ASME International Mechanical Engineering Congress and Exposition*, Dallas, TX.

Aircraft Engineering and Aerospace Technology: An International Journal
Volume 86 · Number 5 · 2014 · 361–374

Walker, D.J. and Voskuijl, M. (2007), "Active control of flight path and critical loads in tilt-rotor aircraft", *American Helicopter Society 63rd Annual Forum*, VA Beach, VA.

Yomchinda, T. (2009), "Integrated flight control design and handling qualities analysis for a tiltrotor aircraft", MS thesis, PA State University, PA.

Yomchinda, T. and Horn, J.F. (2009), "Handling qualities assessment of a model inversion controller for a tiltrotor aircraft", *Proceedings of the 3rd International Basic Research Conference on Rotorcraft Technology*, *Nanjing*.

Yoo, C., Lee, J. and Walker, D.J. (2009), "Design of longitudinal SCAS for tilt rotor aircraft based on H-infinity", *Autumn Conference of Korean Society for Aeronautical and Space Sciences*, *Gyeongju*.

Yu, C., Zhu, J. and Sun, Z. (2005), "Nonlinear adaptive internal model control using neural networks for tiltrotor aircraft platform", *Proceedings of the IEEE Mid-Summer Workshop on Soft Computing in Industrial Applications*, *Finland*, pp. 12-16.

Zhu, G. and Skelton, R.E. (1991), "Mixed L_2 and L_∞ problems by weight selection in quadratic optimal control", *International Journal of Quadratic Optimal Control*, Vol. 63 No. 5, pp. 1161-1176.

Zhu, X.P., Fan, Y.H. and Yang, J. (2010), "Design of tiltrotor flight control system using fuzzy sliding mode control", *International Conference on Measuring Technology and Mechatronics Automation*, *Changsha*.

Appendix

For hover flight condition and 200 kts straight-level flight condition, A and B matrices are given in equations (8a), (8b), (9a) and (9b) (taken from Ferguson, 1983).

Helicopter Mode (hover flight condition)

$$A = \begin{bmatrix} -0.0127 & 0 & -0.0027 & 0 & 1.3154 & 0 & 0 & -32.166 & 0 \\ 0 & -0.057 & 0 & -1.2538 & 0 & -0.487 & 32.1662 & 0 & 0 \\ -0.0707 & 0 & -0.1984 & 0 & 0.3576 & 0 & 0 & 0.4963 & 0 \\ 0 & -0.005 & 0 & -0.3568 & 0 & 0.1159 & 0 & 0 & 0 \\ 0.0007 & 0 & 0 & 0 & -0.2007 & 0 & 0 & 0 & 0 \\ 0 & 0.0012 & 0 & 0.1511 & 0 & -0.0286 & 0 & 0 & 0 \\ 0 & 0 & 0 & 1 & 0 & 0 & 0 & 0 & 0 \\ 0 & 0 & 0 & 0 & 1 & 0 & 0 & 0 & 0 \\ 0 & 0 & 0 & 0 & 0 & 1 & 0 & 0 & 0 \end{bmatrix} \tag{8a}$$

$$B = \begin{bmatrix} 1.33 & -0.0843 & 0 & 0 \\ 0 & 0 & -0.0434 & 0.2446 \\ 0.0154 & -5.3566 & 0 & 0 \\ 0 & 0 & 0.2411 & 0.0232 \\ -0.1887 & -0.0029 & 0 & 0 \\ 0 & 0 & -0.0211 & 0.1006 \\ 0 & 0 & 0 & 0 \\ 0 & 0 & 0 & 0 \\ 0 & 0 & 0 & 0 \end{bmatrix} \tag{8b}$$

Airplane Mode (200 kts straight-level flight condition)

$$A = \begin{bmatrix} -0.4138 & 0 & 0.0729 & 0 & -6.5286 & 0 & -32.1621 & 0 & 0 \\ 0 & -0.3744 & 0 & 6.3158 & 0 & 32.1621 & 0 & 0 & 0 \\ -0.1709 & 0 & -1.2073 & 0 & 325.1683 & 0 & -0.7124 & 0 & 0 \\ 0 & -0.0131 & 0 & -0.8073 & 0 & 0 & 0 & 0 & 0 \\ 0.0215 & 0 & -0.0372 & 0 & -2.1913 & 0 & 0 & 0 & 0 \\ 0 & 0.0096 & 0 & -0.1881 & 0 & 0 & 0 & 0 & 0 \\ 0 & 0 & 0 & 1 & 0 & 0 & 0 & 0 & 0 \\ 0 & 0 & 0 & 0 & 1 & 0 & 0 & 0 & 0 \\ 0 & 0 & 0 & 0 & 0 & 0 & 0 & 0 & 0 \end{bmatrix} \tag{9a}$$

$$B = \begin{bmatrix} -0.0656 & 5.1084 & 0 & 0 \\ 0 & 0 & 0.0041 & -2.7109 \\ -3.1791 & 0.0615 & 0 & 0 \\ 0 & 0 & 0.3339 & -0.0694 \\ -1.4324 & -0.2439 & 0 & 0 \\ 0 & 0 & 0.0902 & 0.3816 \\ 0 & 0 & 0 & 0 \\ 0 & 0 & 0 & 0 \\ 0 & 0 & 0 & 0 \end{bmatrix} \tag{9b}$$

State estimator and control gain matrices

For 1st and 2nd OVCs, the state estimator and gain matrices are found using OVC algorithm (Hsieh *et al.*, 1989; Zhu and Skelton, 1991), and these are:

$$G_{1st\_OVC} = \begin{bmatrix} 2.67e{-}3 & 6.93e{-}18 & 1.31e{-}5 & -1.80e{-}15 & 1.63e{+}1 & -4.86e{-}16 & -3.81e{-}15 & 2.85e{+}1 & -1.45e{-}16 \\ 7.30e{-}5 & 7.00e{-}19 & -1.87e{-}7 & -1.59e{-}16 & 2.53e{-}1 & 3.20e{-}18 & -2.91e{-}16 & 4.38e{-}1 & -4.46e{-}18 \\ -5.25e{-}18 & 1.52e{-}2 & 6.06e{-}18 & -1.14e{+}1 & 2.21e{-}15 & 3.02e{-}2 & -2.00e{+}1 & 2.69e{-}16 & 2.05e{-}1 \\ -2.08e{-}18 & -7.55e{-}3 & 3.82e{-}19 & -1.71 & 4.57e{-}16 & -7.34 & -1.59 & 7.96e{-}17 & -2.89 \end{bmatrix} \quad (10a)$$

$$F_{1st\_OVC} = \begin{bmatrix} 8.31 & 1.94e{-}10 & -2.84e{-}1 & -2.31e{-}11 & -4.47e{-}1 & -6.66e{-}11 & -1.54e{-}10 & -1.10 & 1.35e{-}10 \\ 5.80e{-}16 & 8.23 & 2.58e{-}16 & 3.96e{-}1 & -3.28e{-}16 & 4.75e{-}2 & 1.09 & -1.38e{-}16 & 2.45e{-}2 \\ -2.84e{-}1 & -2.46e{-}11 & 8.60e{-}1 & -5.75e{-}12 & 1.19e{-}1 & 2.81e{-}10 & -2.27e{-}12 & 5.06e{-}2 & 2.47e{-}12 \\ -2.40e{-}16 & 3.96e{-}1 & 1.15e{-}15 & 6.21e{-}1 & 2.59e{-}16 & 8.38e{-}2 & 1.46e{-}1 & 7.43e{-}17 & 3.75e{-}2 \\ -4.47e{-}1 & -6.95e{-}11 & 1.19e{-}1 & -5.92e{-}12 & 6.93e{-}1 & -8.64e{-}11 & -2.50e{-}11 & 1.63e{-}1 & -9.47e{-}11 \\ 2.58e{-}17 & 4.75e{-}2 & 2.43e{-}16 & 8.38e{-}2 & 3.02e{-}17 & 8.94e{-}1 & 3.06e{-}2 & 8.78e{-}18 & 4.06e{-}1 \\ -3.90e{-}16 & 1.09 & 4.03e{-}15 & 1.46e{-}1 & 4.70e{-}16 & 3.06e{-}2 & 2.86e{-}1 & 1.36e{-}16 & 1.50e{-}2 \\ -1.10 & -2.00e{-}10 & 5.06e{-}2 & -3.06e{-}11 & 1.63e{-}1 & -1.38e{-}10 & -7.00e{-}11 & 2.90e{-}1 & -4.95e{-}11 \\ -1.43e{-}17 & 2.45e{-}2 & 1.36e{-}16 & 3.75e{-}2 & 1.68e{-}17 & 4.06e{-}1 & 1.50e{-}2 & 4.89e{-}18 & 1.28 \end{bmatrix} \quad (10b)$$

$$G_{2nd\_OVC} = \begin{bmatrix} 3.86e{-}3 & 3.63e{-}18 & -2.82e{-}3 & -1.73e{-}15 & 1.57e{-}1 & -1.08e{-}15 & -2.93e{-}15 & 1.31 & -2.43e{-}15 \\ -1.45e{-}4 & 2.44e{-}18 & -7.67e{-}5 & -2.21e{-}16 & 1.33e{-}2 & -3.96e{-}17 & -4.24e{-}16 & 6.13e{-}2 & 3.79e{-}16 \\ 7.88e{-}18 & 2.49e{-}2 & -5.37e{-}18 & -5.37 & 4.81e{-}16 & -2.44 & -1.00e{+}1 & 2.37e{-}15 & -4.12e{-}1 \\ 9.27e{-}18 & 7.43e{-}3 & -4.36e{-}18 & -1.27 & 2.19e{-}16 & -2.26 & -5.77e{-}1 & 1.44e{-}15 & -1.13 \end{bmatrix} \quad (11a)$$

$$F_{2nd\_OVC} = \begin{bmatrix} 7.50 & -9.82e{-}11 & -2.33e{-}1 & 2.38e{-}9 & -4.82e{-}3 & -5.90e{-}10 & -6.55e{-}9 & -9.70e{-}1 & 3.87e{-}10 \\ 2.83e{-}16 & 2.42e{+}1 & -3.34e{-}14 & 1.41e{-}1 & -4.57e{-}15 & -8.95e{-}1 & 2.51e{-}1 & 8.78e{-}16 & -6.40e{-}2 \\ -2.33e{-}1 & 3.34e{-}10 & 2.17e{+}1 & -5.99e{-}10 & 8.07e{-}1 & 5.50e{-}11 & 1.52e{-}9 & 4.29e{-}2 & 1.92e{-}10 \\ 1.81e{-}16 & 1.41e{-}1 & 1.28e{-}15 & 4.56e{-}1 & 3.45e{-}16 & 1.37e{-}2 & 1.72e{-}1 & -1.15e{-}16 & 6.03e{-}3 \\ -4.82e{-}3 & -2.96e{-}11 & 8.07e{-}1 & -6.25e{-}11 & 6.50e{-}2 & 8.88e{-}12 & 1.17e{-}10 & 1.31e{-}3 & 1.36e{-}11 \\ -3.57e{-}17 & -8.95e{-}1 & -1.01e{-}16 & 1.37e{-}2 & 7.96e{-}17 & 8.00e{-}2 & 9.34e{-}2 & -2.81e{-}18 & 7.62e{-}3 \\ 8.71e{-}17 & 2.51e{-}1 & 3.24e{-}16 & 1.72e{-}1 & 9.84e{-}17 & 9.34e{-}2 & 1.11 & -3.95e{-}17 & 5.37e{-}2 \\ -9.70e{-}1 & 6.52e{-}11 & 4.29e{-}2 & -7.32e{-}10 & 1.31e{-}3 & 1.71e{-}10 & 1.94e{-}9 & 2.46e{-}1 & -1.34e{-}10 \\ 1.44e{-}19 & -6.40e{-}2 & 9.65e{-}17 & 6.03e{-}3 & 1.65e{-}17 & 7.62e{-}3 & 5.37e{-}2 & -3.40e{-}18 & 1.00 \end{bmatrix} \quad (11b)$$

About the author

Tugrul Oktay received an MS in aeronautical and astronautical engineering from Istanbul Technical University (2009), and he received a PhD for aerospace engineering in the Aerospace and Ocean Engineering Department at Virginia Tech (2012). He had a scholarship from the Ministry of National Education, Republic of Turkey. His main research areas are constrained modern control techniques (e.g. variance constrained control, model predictive control, Hinf control) and stochastic optimization methods (e.g. singular perturbation stochastic approximation). He is also interested in developing sophisticated, control-oriented, physics-based helicopter models. He is currently with Civil Aviation School, Erciyes University. Tugrul Oktay can be contacted at: tugruloktay52@gmail.com